Three-dimensional walking spatiotemporal solitons in quadratic media

Dumitru Mihalache,[1,2] Dumitru Mazilu,[1,2] Lucian-Cornel Crasovan,[2] Lluis Torner,[3] Boris A. Malomed,[4] and Falk Lederer[1]
[1]*Institute of Solid State Theory and Theoretical Optics, Friedrich-Schiller-University Jena, Max-Wien-Platz 1, D-07743, Germany*
[2]*Department of Theoretical Physics, National Institute of Physics and Nuclear Engineering, Institute of Atomic Physics, P.O. Box MG-6, Bucharest, Romania*
[3]*Laboratory of Photonics, Department of Signal Theory and Communications, Polytechnic University of Catalonia, Barcelona, ES 08034, Spain*
[4]*Department of Interdisciplinary Sciences, Faculty of Engineering, Tel Aviv University, Tel Aviv 69978, Israel*
(Received 14 June 2000)

Two-parameter families of chirped stationary three-dimensional spatiotemporal solitons in dispersive quadratically nonlinear optical media featuring type-I second-harmonic generation are constructed in the presence of temporal walk-off. Basic features of these walking spatiotemporal solitons, including their dynamical stability, are investigated in the general case of unequal group-velocity dispersions at the fundamental and second-harmonic frequencies. In the cases when the solitons are unstable, the growth rate of a dominant perturbation eigenmode is found as a function of the soliton wave number shift. The findings are in full agreement with the stability predictions made on the basis of a marginal linear-stability curve. It is found that the walking three-dimensional spatiotemporal solitons are dynamically *stable* in most cases; hence in principle they may be experimentally generated in quadratically nonlinear media.

PACS number(s): 42.81.Dp, 42.65.Ky, 52.35.Sb

I. INTRODUCTION

Solitons in optical media with quadratic nonlinearities exhibit unique dynamical behaviors and have a great potential for applications to photonic devices [1–19]. One of the fundamentally important properties is the fact that, unlike the Kerr nonlinearity [20], the quadratic nonlinearity does not lead to wave collapse in any physical dimension [3], and thus it opens a way to generate stable spatiotemporal solitons (STS's), or ''light bullets'' [20], i.e., fully localized spatiotemporal objects that result from the simultaneous balance of diffraction and dispersion by nonlinear phase modulation. STS's in various types of nonlinear optical environments have attracted a great deal of interest [21–31]. On one hand, STS's are challenging objects for fundamental research, as examples of stable localized objects in two-dimensional (2D) and, especially, in three-dimensional (3D) nonlinear media are rare in physics. On the other hand, STS's hold promise for potential applications in future ultrafast all-optical logic devices, where each STS may represent an elementary bit of information, provided that stable STS's can be formed from pulses at reasonable energy levels in available optical materials.

The formation of 2D STS's in quadratically nonlinear media has recently been observed [32]. In these experiments, tilted-pulse techniques were used to control the effective group-velocity dispersion (GVD) and group-velocity mismatch (GVM) experienced by the propagating signals [33]. In particular, the effective GVD was made anomalous and properly enhanced, while the GVM was reduced. An important peculiarity of the results reported in [32] is that 2D STS's can be successfully generated despite a nonvanishing value of group-velocity mismatch between fundamental-harmonic (FH) and second-harmonic (SH) waves. Very recently, noncollinear generation of optical 2D STS's, based on type-I interaction (that which involves a single FH wave) in quadratically nonlinear media has been demonstrated in a barium metaborate [Ba_2BO_4,(BBO)] crystal [34]. The resulting Y-like geometry of optical STS generation can be used to implement optical logical AND gates with ultrafast high-contrast operation. However, 3D STS's in quadratically nonlinear media have not been observed experimentally thus far.

An important feature that must be taken into consideration in any physically realistic model of second-harmonic generation (SHG) media is the fact that the FH and SH waves have different dispersions: while the dispersion at both frequencies must be anomalous to support fully stationary STS's [25], their absolute values are, generally, different. This implies that equations describing the structure of the STS include a spatiotemporal anisotropy which has no analog in the case of spatial solitons [25].

Static (*nonwalking*) STS's [25–28] are represented by *real* solutions to the corresponding coupled nonlinear wave equations. In this case, STS's actually move at a velocity *exactly* equal to the group velocity of the carrier waves. In the SHG model, it is usually assumed that FH and SH group velocities coincide. Then, the only free parameter of the STS solutions is their propagation constant (nonlinear wave number shift). An important generalization to the case of ''walking'' STS's, represented by *complex* (chirped) stationary solutions, that move at a finite velocity relative to the carrier-wave group velocity, was recently carried out for a simpler 2D case [35]. Such a generalization was necessary, first of all, because, in reality, the FH and SH group velocities are not exactly equal. Moreover, in a real experimental situation, the mismatch between the two group velocities may be significant [32], which does not prevent the formation of quadratic solitons when the phase mismatch between the waves is correspondingly large [36], but makes a detailed theoretical study of the walking effects necessary.

Families of 1D walking solitons have been studied in de-

tail as solitary-wave solutions of the SHG models in the presence of spatial or temporal walkoff [15–17]. It has been found that walking solitons have features essentially different from static ones, e.g., a different energy distribution between their FH and SH components, and different soliton content [37] produced by arbitrary (nonsoliton) input pulses. From the mathematical viewpoint, walking solitons exhibit an extra free parameter in comparison with the static solitary-wave solutions, viz., the above-mentioned velocity of the soliton relative to its carrier-wave's group velocity.

The objective of the present work is to construct a two-parameter family of 3D walking STS's, and test their dynamical stability. The spatiotemporal profile and the stability of the solitons will be studied as a function of the energy, wave number mismatch between the FH and SH waves, and ratio of the SH and FF dispersion coefficients.

The rest of the paper is organized as follows. In Sec. II, the model giving rise to 3D walking STS's is presented in its nonstationary and stationary versions. In the same section, the model's dynamical invariants (integrals of motion), viz., energy, Hamiltonian, and momentum, are considered. In Sec. III, detailed numerical studies of unique features of the two-parameter families of solitons and a comprehensive analysis of their stability is presented. Results obtained in this work are briefly summarized in the final section.

II. TWO-PARAMETER FAMILIES OF WALKING 3D STS'S

The normalized equations describing type-I SHG in a 3D geometry in the presence of chromatic dispersion and GVM can be written as follows (see [4,25]):

$$i\frac{\partial a_1}{\partial \xi}-\frac{r}{2}\left(\frac{\partial^2 a_1}{\partial \eta^2}+\frac{\partial^2 a_1}{\partial \zeta^2}+\frac{\partial^2 a_1}{\partial t^2}\right)+a_1^* a_2\exp(-i\beta\xi)=0,$$

$$i\frac{\partial a_2}{\partial \xi}-\frac{\alpha}{2}\left(\frac{\partial^2 a_2}{\partial \eta^2}+\frac{\partial^2 a_2}{\partial \zeta^2}+\sigma\frac{\partial^2 a_2}{\partial t^2}\right)-i\delta\frac{\partial a_2}{\partial t}+a_1^2\exp(i\beta\xi)=0. \quad (1)$$

Here, ξ, η, ζ, and t are, respectively, the normalized propagation (longitudinal) coordinate, the two transverse spatial coordinates, and the so-called retarded time, whereas a_1 and a_2 are the FH and SH fields, δ is the GVM parameter (the spatial walk-off can be neglected if we assume noncritical or quasi-phase matching), $\alpha=-k_1/k_2\simeq-0.5$, where $k_{1,2}$ are linear wave numbers at both frequencies, and δ is the GVM parameter. For the FH, anomalous dispersion is assumed, hence we set $r=-1$. The parameter β stands for the phase mismatch between the two waves, and σ is the dispersion parameter ($-\alpha\sigma$ being the ratio of the SH and FH dispersion coefficients). The dispersion parameter σ may have any sign (but solitons exist only if the SH dispersion is also anomalous or exactly zero, i.e., $\sigma\geqslant 0$ [25]). In the case $\sigma=1$, Eqs. (1) feature a formal spherical isotropy.

We are looking for stationary solutions to Eqs. (1) describing mutually trapped FH and SH pulses walking off the ξ axis; hence we set

$$a_{1,2}(\xi,\eta,\zeta,t)=U_{1,2}(\eta,\zeta,\tau)\exp[i\phi_{1,2}(\xi,\eta,\zeta,\tau)], \quad (2)$$

$U_{1,2}(\eta,\zeta,\tau)$ and $\phi_{1,2}(\xi,\eta,\zeta,\tau)$ being real functions, where $\tau\equiv t-v\xi$ is the normalized ''reduced time'' in the reference frame moving (along with the soliton) at an inverse velocity v relative to the laboratory frame, and the phases are sought for as $\phi_{1,2}=\kappa_{1,2}\xi+f_{1,2}(\eta,\zeta,\tau)$. Here, v is the soliton velocity, $\kappa_{1,2}$ are nonlinear wave number shifts, and the functions $f_{1,2}(\eta,\zeta,\tau)$ describe a transverse structure of the soliton phase front. To obtain ξ-independent stationary solutions, one needs to set $\kappa_2=2\kappa_1+\beta$. The amplitudes $U_{1,2}(\eta,\zeta,\tau)$ and the phase-front functions $f_{1,2}(\eta,\zeta,\tau)$ satisfy the following symmetry properties: $U_{1,2}(\eta,\zeta,\tau)$ are even functions of all the transverse variables (η,ζ,τ), while $f_{1,2}(\eta,\zeta,\tau)$ are even functions of (η,ζ) and odd functions of τ.

In order to find steady-shape walking solitons, we solved numerically the following coupled system of equations, using a standard band-matrix method [38] to deal with the corresponding two-point boundary-value problem:

$$-\frac{r}{2}\left(\frac{\partial^2 u_1}{\partial \eta^2}+\frac{\partial^2 u_1}{\partial \zeta^2}+\frac{\partial^2 u_1}{\partial \tau^2}\right)-iv\frac{\partial u_1}{\partial \tau}-\kappa_1 u_1+u_1^* u_2=0,$$

$$-\frac{\alpha}{2}\left(\frac{\partial^2 u_2}{\partial \eta^2}+\frac{\partial^2 u_2}{\partial \zeta^2}+\sigma\frac{\partial^2 u_2}{\partial \tau^2}\right)-i(\delta+v)\frac{\partial u_2}{\partial \tau}-(2\kappa_1+\beta)u_2+u_1^2=0, \quad (3)$$

where the unknown complex functions are split into real amplitudes and phases,

$$u_{1,2}(\eta,\zeta,\tau)\equiv U_{1,2}(\eta,\zeta,\tau)\exp[if_{1,2}(\eta,\zeta,\tau)].$$

The associated system of nonlinear equations obtained from the second-order finite-difference approximation to the system (3) was solved by the Newton method. In Eqs. (3) α, β, and δ are the model parameters, while the nonlinear wave number shift κ_1 and the velocity v parametrize the family of stationary walking STS's. In the absence of temporal walk-off, one has $\delta=0$, and zero-velocity soliton solutions to the above equations are known to exist [25,26,28].

In what follows below, we make use of the fact that Eqs. (1) give rise to three conserved quantities (integrals of motion): the energy (number of photons) I, Hamiltonian H, and momentum J,

$$I\equiv I_1+I_2=\int(|A_1|^2+|A_2|^2)d\eta d\zeta dt, \quad (4)$$

$$H=-\frac{1}{2}\int\left[r\left(\left|\frac{\partial A_1}{\partial\eta}\right|^2+\left|\frac{\partial A_1}{\partial\zeta}\right|^2+\left|\frac{\partial A_1}{\partial t}\right|^2\right)+\frac{\alpha}{2}\left(\left|\frac{\partial A_2}{\partial\eta}\right|^2+\left|\frac{\partial A_2}{\partial\zeta}\right|^2+\sigma\left|\frac{\partial A_2}{\partial t}\right|^2\right)-\beta|A_2|^2+i\frac{\delta}{2}\left(A_2\frac{\partial A_2^*}{\partial t}-A_2^*\frac{\partial A_2}{\partial t}\right)+(A_1^{*2}A_2+A_1^2A_2^*)\right]d\eta d\zeta dt, \tag{5}$$

$$J\equiv J_1+J_2=\frac{1}{4i}\int\left[2\left(A_1^*\frac{\partial A_1}{\partial t}-A_1\frac{\partial A_1^*}{\partial t}\right)+\left(A_2^*\frac{\partial A_2}{\partial t}-A_2\frac{\partial A_2^*}{\partial t}\right)\right]d\eta d\zeta dt, \tag{6}$$

where we have defined $A_1\equiv a_1$ and $A_2\equiv a_2\exp(-i\beta\xi)$.

The steady-shape walking STS's of the form given by Eq. (2) occur as extrema of the Hamiltonian at fixed energy and transverse momentum:

$$\delta_F(H+\kappa_1 I-vJ)=0, \tag{7}$$

δ_F standing for the variational derivative. By directly manipulating the governing equations (1), one finds that the walking soliton solutions correspond to a value of the Hamiltonian

$$H=-\frac{1}{3}\kappa_1 I+\frac{1}{3}\beta I_2+\frac{2}{3}vJ-\frac{1}{3}\delta J_2. \tag{8}$$

When $\delta=0$, the last two terms on the right-hand side of this expression vanish for the zero-velocity solutions. However, in the presence of group-velocity mismatch ($\delta\neq 0$), only the third term vanishes for the zero-velocity solitons, whereas the last term contributes to the Hamiltonian. This is an indication that the transverse momentum of walking solitons is not simply proportional to their velocity, in contrast with the walking soliton solutions to Galilean-invariant equations. Substitution of Eq. (2) into Eq. (6) yields

$$J=\frac{1}{2}\int(2U_1^2\dot{f}_1+U_2^2\dot{f}_2)d\eta d\zeta d\tau, \tag{9}$$

where the overdots stand for the derivative with respect to τ. If traveling-wave solutions can be trivially generated by the Galilean transformation (in a Galilean-invariant model), the derivatives $\dot{f}_{1,2}$ are constant, $\dot{f}_1=v$ and $\dot{f}_2=-(\delta+v)/(\alpha\sigma)$. In general, for walking solitons, these derivatives are not simply proportional to the velocity, and hence neither is J. A relation between velocity and momentum for steady walking STS's can be elucidated by examining the evolution of the energy centroid of the coupled copropagating FH and SH fields. One thus finds

$$J=vI+\delta I_2+(2\alpha\sigma+1)J_2. \tag{10}$$

The second term on the right-hand side of Eq. (10) stands for the so-called dragging effect, that is, mutual dragging of the FH and SH components [11]. We notice that from Eq. (10) one can find an estimate for the eventual velocity of the walking STS's generated by arbitrary input pulses, provided that the radiation losses may be neglected.

In order to find the existence condition for walking STS's, we notice that steady-shape walking soliton solutions to Eqs. (3) exist for values of the nonlinear wave number shifts κ_1 and transverse velocities v such that the soliton is not in resonance with the linear dispersive waves, to avoid energy leakage from the soliton. We find that the corresponding cutoff (limit) value of the FH wave number shift is $\kappa_{1,\mathrm{cutoff}}^{(1)}=(1/2)v^2$, whereas the resonance of the SH soliton component with the linear dispersive waves occurs for wave numbers below $\kappa_{1,\mathrm{cutoff}}^{(2)}=(\delta+v)^2/4(-\alpha)\sigma-\beta/2$. Thus, stationary walking STS's exist for values of the nonlinear wave number shift κ_1 above both these cutoffs. We also note that, in 1D SHG models, so-called embedded solitons may exist, which are isolated solitary waves (i.e., they do not exist in families) avoiding resonance with dispersive waves in the FH component but located inside the continuous spectrum of the SH waves, and may be semistable (linearly stable but unstable in the nonlinear approximation) [39]. It is not ruled out that embedded solitons are also possible in the spatiotemporal domain, but this problem is beyond the scope of this work.

Next we consider the condition for linear (marginal) stability of the two-parameter families of STS's. By using a multiscale asymptotic approach [13,16,35], the marginal linear-stability curve is given by

$$\frac{\partial I}{\partial\kappa_1}\frac{\partial J}{\partial v}-\frac{\partial I}{\partial v}\frac{\partial J}{\partial\kappa_1}=0. \tag{11}$$

Notice that the condition (11) is only a *sufficient* criterion for instability and it can also be derived by using geometrical methods [40].

III. NUMERICAL RESULTS

In the numerical calculations, we have fixed the value of the GVM parameter $\delta=1$ and set $\alpha=-0.5$ [recall that the parameter r in Eqs. (1) was already chosen to be -1, i.e., we consider the case when the dispersion is anomalous at both frequencies]. In Fig. 1, we plot the energy dependence of the wave number shift κ_1 and Hamiltonian H for both negative and positive values of the phase mismatch β, several different values of the soliton velocity v, and a typical value of the relative dispersion parameter σ. Because the curves plotted in Fig. 1 correspond to fixed soliton velocities, the momentum J is not constant along the curves. This explains the fact that it is possible to have stable solitons for a fixed value of energy and different values of the Hamiltonian, as is seen in Fig. 1(d). As in the case of static (nonwalking) 3D STS's [26,28], 3D walking STS's are unstable for both signs of the phase mismatch, but only in a narrow interval of the wave numbers near cutoff (see the dashed lines in Fig. 1). This result should be compared to the stability of nonwalking [27] and walking (for certain choices of the dispersion parameter σ) [35] 2D STS's in the whole range of their existence at positive mismatches.

For the sake of comparison, we have plotted in Figs. 2 the energy dependence of the wave number shift κ_1 and of the Hamiltonian H, at a fixed value of the soliton velocity v, for

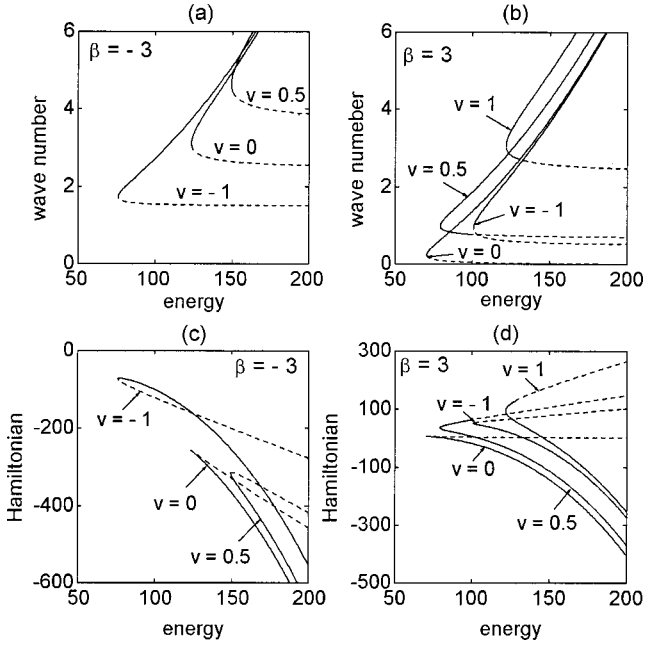

FIG. 1. (a) and (b) The wave number shift κ_1 vs the energy I; (c) and (d) the Hamiltonian H vs the energy I. Here $\sigma=0.5$; the other parameters are indicated on the plots. The continuous and dashed lines correspond to stable and unstable solitons, respectively.

two representative values of phase mismatches and for several values of the dispersion parameter σ. As in Fig. 1, we notice that the momentum J is not constant along the curves plotted in Fig. 2. A majority of walking STS's are dynamically stable, except the ones close to the cutoff, plotted by the dashed lines in Figs. 1 and 2. In all cases plotted in Figs. 1 and 2, the threshold energy is determined numerically and corresponds to a point where $\partial I/\partial\kappa_1=0$. Notice that, in some regions of the parameter values, the threshold energy

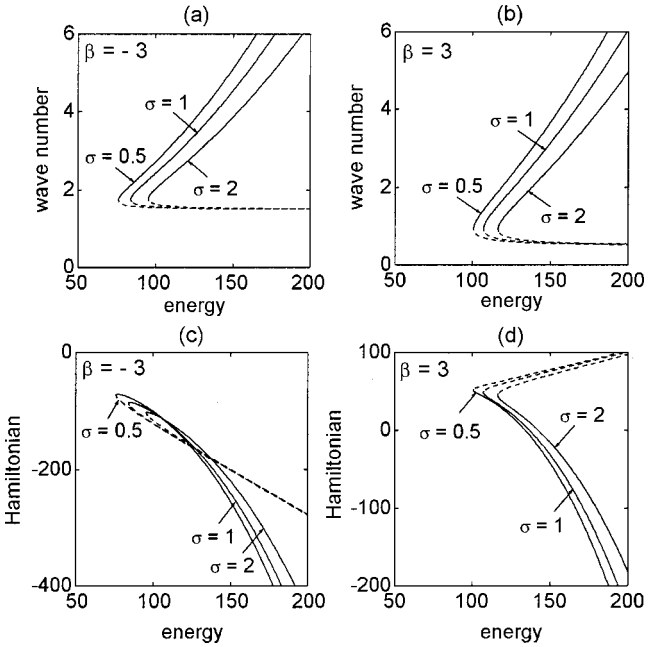

FIG. 2. The same as in Fig. 1, but with $v=-1$. The other parameters are indicated on the plots.

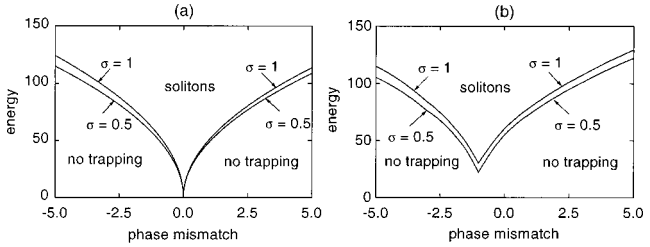

FIG. 3. Threshold energy for the formation of the spatiotemporal soliton vs β. (a) $\delta=0$; (b) $\delta=1$. Here, $v=-1$.

more than doubles in the interval of variation of the velocity (see Fig. 1). For our choice of the parameters, we notice that the energy threshold for the formation of walking STS's depends monotonically on the soliton velocity [see Fig. 1(a)] for negative phase mismatch β, whereas at positive phase mismatch the dependence of the energy threshold is not monotonic [see Fig. 1(b)]. When we fix the value of the velocity as in Fig. 2, we find that this threshold monotonically increases with increase of the dispersion parameter σ, regardless of the sign of the phase mismatch β.

In Fig. 3 we plot the threshold energy for 3D STS formation as a function of the phase mismatch β for both nonwalking [Fig. 3(a)] and walking STS's [Fig. 3(b)]. Here we have fixed a representative value of the velocity ($v=-1$) of the walking STS. At the exact-phase-matching point ($\beta=0$), the energy threshold for nonwalking STS's vanishes, regardless of the relative dispersion σ, and as the phase mismatch is increased more energy is needed for the formation of 3D STS's. Note that low-energy STS's have large widths, which is a common property of solitons irrespective of the space dimension.

When δ (the GVM parameter) is zero, the threshold energy scales as $|\beta|^{1/2}$, regardless of the relative dispersion parameter σ, and at negative phase mismatch it is larger than at positive phase mismatch [see Fig. 3(a)], in accordance with the well-known fact that, at large negative phase mismatch, the wave-mixing process in a quadratically nonlinear medium can be viewed as giving rise to an effective self-defocusing cubic nonlinearity for the fundamental harmonic, whereas at large positive phase mismatch the effective cubic nonlinearity is of a self-focusing type. We see from Fig. 3(b) that in the case of walking 3D STS's the energy threshold is very asymmetric as a function of the phase mismatch parameter β. Moreover, in order to form a walking STS, one has a nonzero threshold even at exact phase matching. As in the case of nonwalking STS's, the threshold energy also depends on the relative dispersion σ.

Now, we are ready to briefly discuss the implications of the Hamiltonian structure [41,42] for the stability of the steady-shape walking STS. The evolution equations (1) can be written in a canonical variational form, and the stationary solitons correspond to extrema of the Hamiltonian for given energy and momentum. As a consequence, the stability of the stationary solutions can be elucidated by taking into account that a global minimum of H gives stable STS's, whereas local maxima yield unstable ones. In the case of smooth surfaces, the marginal stability curve given by Eq. (11) separates the lower and upper sheets of the surface. This is not necessarily the case for nonsmooth surfaces, for in-

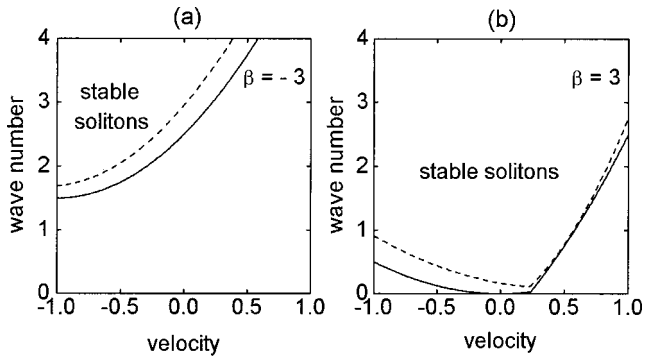

FIG. 4. Domains of soliton existence and stability in the parameter plane (v,κ_1). Here, $\delta=1$ and $\sigma=0.5$.

stance, those found in the case of nonwalking solitons supported by type-II SHG [43].

Figure 4 is a summary of the stability analysis results for the two-parameter family of solitons that exists at $\beta=\mp 3$, $\delta=1$, and $\sigma=0.5$, with the velocity in the range $-1\leqslant v\leqslant 1$. The values of the nonlinear wave number shift κ_1 corresponding to the cutoff for the soliton existence, and to the marginal stability condition given by Eq. (11), are shown, respectively, by the full and dashed curves. Above the dashed curves in Fig. 4, all 3D STS's are stable, whereas unstable ones occur in a narrow region between the cutoff and marginal-stability curves. It is seen from this figure that, at negative phase mismatch, the domain of the existence and stability of 3D STS's shrinks considerably in comparison with the case of positive phase mismatch.

In order to give an idea of the shape of the surface $H=H(I,J)$ for two selected values of the mismatch parameter β, we show a few curves of constant velocity lying on this surface, viz., the dotted lines in Figs. 5(a), (b). The marginal curve separating the stable and unstable sheets of the surface $H=H(I,J)$ is also plotted [the full lines in Figs. 5(a),(b)].

Direct numerical simulations of Eqs. (1) with the input conditions taken as per the steady-shape walking STS at several characteristic sets of the parameter values have confirmed the dynamical stability of the solitons belonging to the lower sheet of the surface $H=H(I,J)$, whereas, in the course of evolution, the unstable solitons on the upper sheet either spread out or reshape themselves into a stable oscillating state close to a stationary walking STS belonging to the lower sheet of the surface (cf. the stable oscillatory states close to nonwalking 3D STS's in the SHG medium that were found in [28]).

A challenging issue is the possibility of an oscillatory instability, accounted for by possible complex eigenvalues generated by the linearization of Eqs. (1) (such an instability was, e.g., found for two-parameter families of solitons in cubic nonlinear media [44]). The numerical problem of finding eigenvalues of the matrix operator generated by the linearization of Eqs. (1) is of formidable complexity and requires huge computational facilities. Notice, however, that the continuum spectrum of the corresponding operator lies on the imaginary axis, namely, on the rays $(\lambda_c, i\infty)$ and $(-\lambda_c, -i\infty)$, where

$$\lambda_c = i \ \min\left\{\kappa_1 - \frac{1}{2}v^2, 2\kappa_1+\beta-\frac{(\delta+v)^2}{(-2\alpha)\sigma}\right\}, \qquad (12)$$

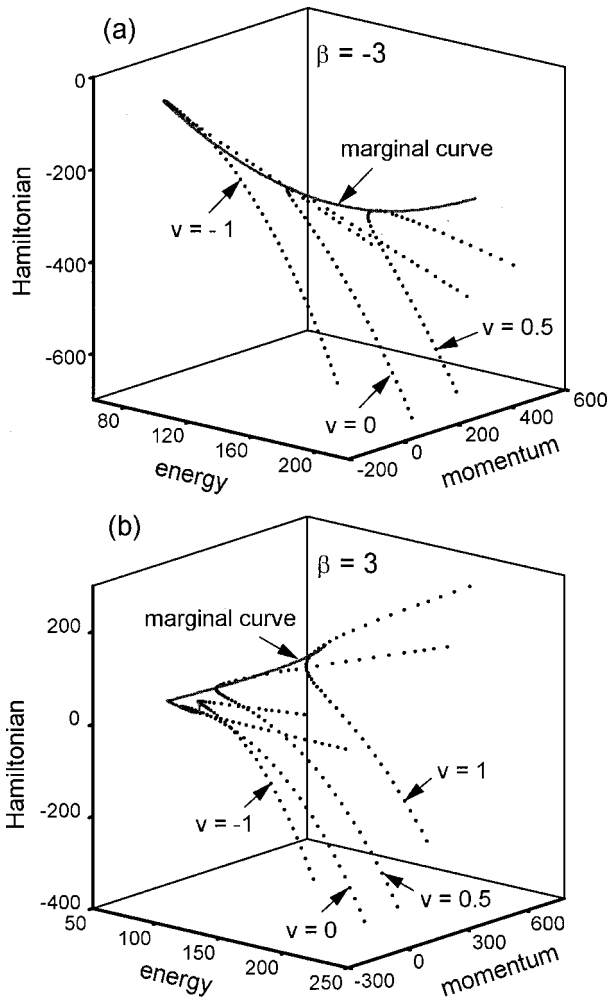

FIG. 5. The surface $H=H(I,J)$ for $\beta=-3$ (a), and for $\beta=3$ (b). Here, $\delta=1$ and $\sigma=0.5$.

as in the case of the two-parameter family of type-I 1D walking solitons in quadratically nonlinear media [16]. Based on the results reported in Ref. [16] for 1D walking solitons, and in Ref. [28] for 2D and 3D nonwalking ones, we also expect to have a nontrivial internal mode in the spectrum below the border of the continuum spectrum. The corresponding pair of eigenvalues may be either real or purely imaginary; thus we expect that oscillatory instabilities do not occur in the present model.

Instead of solving the eigenvalue problem directly we have used the method of obtaining the growth rates of dominant perturbation eigenmodes described, e.g. in Refs. [45,46]. This powerful method has been employed recently in the study of stability of higher-order bound states in saturable self-focusing media [45,46] and in the study of azimuthal instability of bright vortex solitons in quadratically nonlinear media [47]. The outcome of such growth-rate calculations is shown in Fig. 6 for a typical value of the soliton velocity $(v=-1)$ and for different values of the relative dispersion σ. The standard numerical method described in detail in Ref. [46] permits calculation of both real and imaginary parts of the dominant perturbation eigenvalue. We have found that this dominant eigenvalue has its imaginary part equal to zero, in accordance with previous calculations in the case of 1D walking solitons [16] and 2D and 3D nonwalking

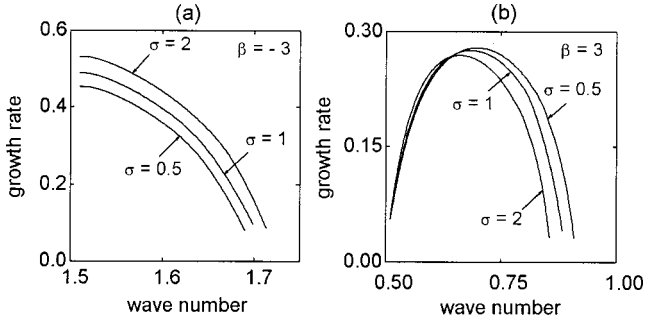

FIG. 6. The instability growth rate of the dominant perturbation vs soliton wave number. (a) $\beta=-3$, (b) $\beta=3$. Here, $v=-1$ and the values of the relative dispersion σ are indicated near the curves.

solitons [28]. We see from Fig. 6 that the maximum growth rates, as a function of the wave number shift κ_1, display different behaviors for the two signs of the phase mismatch. The calculations of the maximum growth rate displayed in Fig. 6 prove to be in full agreement with the stability results obtained from the analysis of the marginal stability curve [see Eq. (11)] that is shown in Fig. 4.

A typical spatiotemporal profile of a stable walking STS at negative phase mismatch is shown in Fig. 7. Here, the parameters are $\beta=-3$, $v=-1$, $I=90$, and $\sigma=0.5$. Because the relative dispersion $\sigma\neq 1$, the soliton displays a spatiotemporal asymmetry (ellipticity [28]).

Next, we display a typical unstable propagation of walking STS's. We have found that our selected numerical simulations are all consistent with the stability criterion (11). We have used the Crank-Nicholson scheme as a finite-difference approximation to Eqs. (1). The corresponding system of nonlinear equations was solved by means of the Picard iteration method (see details in Ref. [48]). Typically, we chose the longitudinal grid size $\Delta\xi=0.02$ and equal transverse grid sizes $\Delta\eta=\Delta\zeta=\Delta\tau=0.10$. The transverse integration window size depends on the choice of the input parameters I and κ_1. The walking STS's are unstable near their existence cutoff (see Figs. 1 and 2). In this region of the parameter space, the stationary STS is rather wide; hence, to exclude possible boundary effects, large computation windows are needed. In Fig. 8 we show snapshots of both the FH and SH components of unstable STS's after propagating over 60 normalized length units. A typical example of an initially unstable STS evolution is displayed in Fig. 9. The propagation takes place in the reference frame in which the initial STS is at rest. We see from Fig. 9 that, during the propagation, the soliton changes its velocity and reshapes itself into a stable near-STS oscillating state. Persistent oscillations of the STS peak amplitude, seen in Fig. 9, are due to both the interaction of the soliton

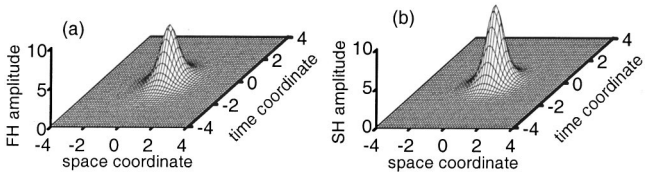

FIG. 7. The spatiotemporal profile of a stable walking soliton. (a) The fundamental harmonic, and (b) the second harmonic. Here, $\beta=-3$, $\kappa_1=2.34$, $\sigma=0.5$, $v=-1$, and $I=90$.

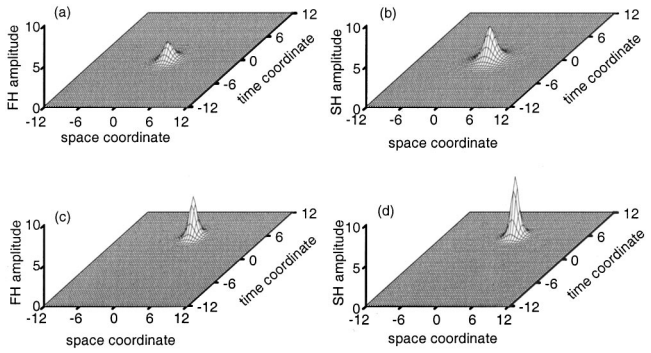

FIG. 8. The spatiotemporal profile of an unstable walking soliton. (a) The fundamental harmonic at $\xi=0$, (b) the second harmonic at $\xi=0$, (c) the fundamental harmonic at $\xi=60$, and (d) the second harmonic at $\xi=60$. Here, $\kappa_1=1.56$, and the other parameters are the same as in Fig. 7.

internal mode [14,36,49]. Notice that the ''oscillating'' nature of many solitons in optical media with $\chi^{(2)}$ nonlinearity, observed when they are either perturbed or generated from arbitrary input pulses, was stressed as their characteristic feature in Ref. [36] for 1D and 2D geometries in the case of equal dispersions at both frequencies, and further confirmed in Ref. [28] for 3D geometries in the general case of unequal dispersions at the two harmonics.

Finally, we mention that other issues of interest that are left beyond the scope of the present work are the generation of walking STS's from, e.g., Gaussian chirped input pulses, the so-called soliton content [37] of an arbitrary input pulse in the same 3D geometry as that considered in the present work, and comprehensive analysis of internal modes of STS solitons.

IV. CONCLUSIONS

In this work, we have studied in detail two-parameter families of stationary three-dimensional walking spatiotem-

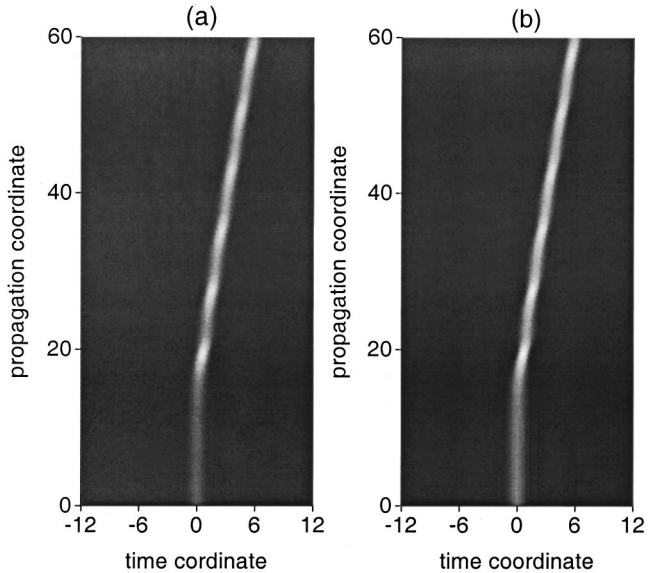

FIG. 9. Gray-scale plots of unstable evolution of the walking soliton. (a) The fundamental harmonic, and (b) the second harmonic. The parameters are the same as in Fig. 8.

poral solitons propagating in dispersive optical media featuring type-I second-harmonic generation. The temporal walk-off between the fundamental and second-harmonic waves was explicitly taken into regard. Parameters characterizing the soliton family are the nonlinear wave number shift and the velocity of the soliton walk-off relative to its carrier waves. These walking ''light bullets'' are fully localized in all three dimensions (two spatial transverse dimensions and the temporal one). The general analysis of three-dimensional walking spatiotemporal solitons is necessary because, by and large in practice, the actual group velocities at the fundamental and second-harmonic frequencies do not coincide (which, however, does not prevent formation of two-dimensional walking spatiotemporal solitons in a real experiment [32]).

We have investigated the properties of chirped walking spatiotemporal solitons, including their dynamical stability, in the general case of unequal group-velocity dispersions at the fundamental and second-harmonic frequencies. The transverse shapes of the three-dimensional light bullets exhibit a spatiotemporal asymmetry.

A detailed numerical analysis of the consequences of the sufficient linear-stability criterion for solitons, found from simple geometrical arguments, was given. In the cases when the spatiotemporal solitons are unstable, the corresponding maximum growth rates have been calculated as functions of the nonlinear wave number in the general case of unequal group-velocity dispersions at the fundamental and second-harmonic frequencies. It was found that, excluding a tiny region near the cutoff of their existence, the walking three-dimensional spatiotemporal solitons are *dynamically stable*.

ACKNOWLEDGMENTS

D.M. and D.M. acknowledge grants from the Deutsche Forschungsgemeinshaft (DFG), Bonn. We are indebted to Frank Wise for valuable discussions and for sending us his work prior to publication.

[1] G. I. Stegeman, D. J. Hagan, and L. Torner, Opt. Quantum Electron. **28**, 1691 (1996); Yu. S. Kivshar, in *Advanced Photonics with Second-Order Optically Nonlinear Processes*, edited by A. D. Boardman, L. Pavlov, and S. Panev (Kluwer Academic, Dordrecht, 1998), p. 451; L. Torner, in *Beam Shaping and Control with Nonlinear Optics*, edited by F. Kajzar and R. Reinisch (Plenum, New York, 1998), p. 229; P. D. Drummond, K. V. Kheruntsyan, and H. He, J. Opt. B: Quantum Semiclass. Opt. **1**, 387 (1999); B. Malomed, in *Nonlinear Science at the Dawn of the 21st Century*, edited by P. L. Christiansen, M. P. Sorensen, and A. C. Scott (Springer, Berlin, 2000), pp. 247–262.

[2] Yu. N. Karamzin and A. P. Sukhorukov, Zh. Éksp. Teor. Fiz. **68**, 834 (1975) [Sov. Phys. JETP **41**, 414 (1975)].

[3] A. A. Kanashov and A. M. Rubenchik, Physica D **4**, 122 (1981).

[4] C. R. Menyuk, R. Schiek, and L. Torner, J. Opt. Soc. Am. B **11**, 2434 (1994).

[5] A. V. Buryak and Y. S. Kivshar, Opt. Lett. **19**, 1612 (1994); Phys. Lett. A **197**, 407 (1995).

[6] L. Torner, C. R. Menyuk, and G. I. Stegeman, Opt. Lett. **19**, 1615 (1994); L. Torner, Opt. Commun. **114**, 136 (1995).

[7] A. V. Buryak, Y. S. Kivshar, and V. V. Steblina, Phys. Rev. A **52**, 1670 (1995).

[8] L. Torner, D. Mihalache, D. Mazilu, E. M. Wright, E. W. Torruellas, and G. I. Stegeman, Opt. Commun. **121**, 149 (1995).

[9] S. K. Turitsyn, Pis'ma Zh. Éksp. Teor. Fiz. **61**, 458 (1995) [JETP Lett. **61**, 469 (1995)].

[10] L. Bergé, V. K. Mezentsev, J. J. Rasmussen, and J. Wyller, Phys. Rev. A **52**, R28 (1995); L. Bergé, O. Bang, J. J. Rasmussen, and V. K. Mezentsev, Phys. Rev. E **55**, 3555 (1997).

[11] L. Torner, W. E. Torruellas, G. I. Stegeman, and C. R. Menyuk, Opt. Lett. **20**, 1952 (1995).

[12] A. De Rossi, S. Trillo, A. V. Buryak, and Y. S. Kivshar, Opt. Lett. **22**, 868 (1997).

[13] D. E. Pelinovsky, A. V. Buryak, and Y. S. Kivshar, Phys. Rev. Lett. **75**, 591 (1995); A. V. Buryak, Y. S. Kivshar, and S. Trillo, *ibid.* **77**, 5210 (1996).

[14] C. Etrich, U. Peschel, F. Lederer, B. A. Malomed, and Y. S. Kivshar, Phys. Rev. E **54**, 4321 (1996).

[15] L. Torner, D. Mazilu, and D. Mihalache, Phys. Rev. Lett. **77**, 2455 (1996); L. Torner, D. Mihalache, D. Mazilu, M. C. Santos, and N. N. Akhmediev, J. Opt. Soc. Am. B **15**, 1476 (1998).

[16] C. Etrich, U. Peschel, F. Lederer, and B. A. Malomed, Phys. Rev. E **55**, 6155 (1997); C. Etrich, U. Peschel, F. Lederer, D. Mihalache, and D. Mazilu, Opt. Quantum Electron. **30**, 881 (1998).

[17] D. Mihalache, D. Mazilu, L.-C. Crasovan, and L. Torner, Opt. Commun. **137**, 113 (1997); Phys. Rev. E **56**, R6294 (1997).

[18] W. C. K. Mak, B. A. Malomed, and P. L. Chu, Phys. Rev. E **55**, 6134 (1997).

[19] P. D. Drummond and H. He, Phys. Rev. A **56**, R1107 (1997); K. V. Kheruntsyan and P. D. Drummond, *ibid.* **58**, 2488 (1998).

[20] Y. Silberberg, Opt. Lett. **15**, 1282 (1990).

[21] D. E. Edmundson and R. H. Enns, Opt. Lett. **17**, 586 (1992).

[22] R. McLeod, K. Wagner, and S. Blair, Phys. Rev. A **52**, 3254 (1995); S. Blair and K. Wagner, Opt. Quantum Electron. **30**, 697 (1998).

[23] Y. Chen and J. Atai, Opt. Lett. **20**, 133 (1995).

[24] H. He, M. J. Werner, and P. D. Drummond, Phys. Rev. E **54**, 896 (1996).

[25] B. A. Malomed, P. Drummond, H. He, A. Berntson, D. Anderson, and M. Lisak, Phys. Rev. E **56**, 7425 (1997).

[26] D. V. Skryabin and W. J. Firth, Opt. Commun. **148**, 79 (1998).

[27] D. Mihalache, D. Mazilu, B. A. Malomed, and L. Torner, Opt. Commun. **152**, 365 (1998).

[28] D. Mihalache, D. Mazilu, J. Dörring, and L. Torner, Opt. Commun. **159**, 129 (1999).

[29] M. Blaauboer, B. A. Malomed, and G. Kurizki, Phys. Rev. Lett. **84**, 1906 (2000); M. Blaauboer, G. Kurizki, and B. A. Malomed, Phys. Rev. E **62**, R57 (2000).

[30] S. Raghavan and G. P. Agrawal, Opt. Commun. **180**, 377 (2000).

[31] I. V. Mel'nikov, D. Mihalache, and N.-C. Panoiu, Opt. Commun. **181**, 345 (2000).

[32] X. Liu, L. J. Qian, and F. W. Wise, Phys. Rev. Lett. **82**, 4631 (1999); X. Liu, K. Beckwitt, and F. Wise, Phys. Rev. E **62**, 1328 (2000).
[33] P. Di Trapani, D. Caironi, G. Valiulis, A. Dubietis, R. Danielius, and A. Piskarskas, Phys. Rev. Lett. **81**, 570 (1998); G. Valiulis, A. Dubietis, R. Danielius, D. Caironi, A. Visconti, and P. Di Trapani, J. Opt. Soc. Am. B **16**, 722 (1999).
[34] X. Liu, K. Beckwitt, and F. Wise, Phys. Rev. E **61**, R4722 (2000).
[35] D. Mihalache, D. Mazilu, B. A. Malomed, and L. Torner, Opt. Commun. **169**, 341 (1999).
[36] L. Torner, C. R. Menyuk, and G. I. Stegeman, J. Opt. Soc. Am. B **12**, 889 (1995); L. Torner and E. M. Wright, *ibid.* **13**, 864 (1996).
[37] L. Torner, J. P. Torres, D. Artigas, D. Mihalache, and D. Mazilu, Opt. Commun. **164**, 151 (1999).
[38] G. Dahlquist and Å. Björk, *Numerical Methods* (Prentice Hall, Englewood Cliffs, NJ, 1974).
[39] J. Yang, B. A. Malomed, and D. J. Kaup, Phys. Rev. Lett. **83**, 1958 (1999); A. R. Champneys and B. A. Malomed, Phys. Rev. E **61**, 886 (2000).
[40] F. V. Kusmartsev, Phys. Rep. **183**, 1 (1989).
[41] E. A. Kuznetsov, A. M. Rubenchik, and V. E. Zakharov, Phys. Rep. **142**, 103 (1986).
[42] N. N. Akhmediev and A. Ankiewicz, *Solitons: Nonlinear Pulses and Beams* (Chapman and Hall, London, 1997).
[43] A. V. Buryak and Y. S. Kivshar, Phys. Rev. Lett. **78**, 3286 (1997).
[44] A. De Rossi, C. Conti, and S. Trillo, Phys. Rev. Lett. **81**, 85 (1998); D. Mihalache, D. Mazilu, and L. Torner, *ibid.* **81**, 4353 (1998).
[45] N. N. Akhmediev, V. I. Korneev, Yu. V. Kuz'menko, Zh. Éksp. Teor. Fiz. **88**, 107 (1985) [Sov. Phys. JETP **61**, 62 (1985)]; J. M. Soto-Crespo, D. R. Heatley, E. M. Wright, and N. N. Akhmediev, Phys. Rev. A **44**, 636 (1991); J. Atai, Y. Chen, and J. M. Soto-Crespo, *ibid.* **49**, R3170 (1994).
[46] D. E. Edmundson, Phys. Rev. E **55**, 7636 (1997).
[47] L. Torner and D. V. Petrov, Electron. Lett. **33**, 608 (1997); W. J. Firth and D. V. Skryabin, Phys. Rev. Lett. **79**, 2450 (1997); D. V. Petrov and L. Torner, Opt. Quantum Electron. **29**, 1037 (1997); D. V. Skryabin and W. J. Firth, Phys. Rev. E **58**, 3916 (1998).
[48] J. M. Ortega, W. C. Rheinboldt, *Iterative Solution of Nonlinear Equations in Several Variables* (Academic Press, New York, 1970), p. 182.
[49] Y. S. Kivshar, D. E. Pelinovsky, T. Cretegny, and M. Peyrard, Phys. Rev. Lett. **80**, 5032 (1998); D. E. Pelinovsky, Y. S. Kivshar, and V. V. Afanasjev, Physica D **116**, 121 (1998); D. E. Pelinovsky, J. E. Sipe, and J. Yang, Phys. Rev. E **59**, 7250 (1999).